HYDROGEOLOGY OF FRACTURED AQUIFERS: APPLICATION OF CONSISTENCY INDEXES FOR THE VALIDATION OF GEOSPATIAL MATHEMATICAL MODELS

HIDROGEOLOGIA DE AQUÍFEROS FRATURADOS: APLICAÇÃO DE ÍNDICES DE CONSISTÊNCIA PARA A VALIDAÇÃO DE MODELOS MATEMÁTICOS GEOESPACIAIS

Tiago DE VARGAS[1], Rossano BELLADONA[2], Maria Eduarda Ribeiro de SOUZA[2]

[1]Instituto de Pesquisas Hidráulicas (UFRGS). Avenida Bento Gonçalves, 9500 - Prédio 44302 - Agronomia, Porto Alegre - RS.
E-mail: tiago.devargas@ufrgs.br
[2]Serviço Autônomo Municipal de Água e Esgoto (SAMAE), Rua Nestor Moreira, 719 - Nossa Senhora de Lourdes, Caxias do Sul.
E-mails: rbelladona@samaecaxias.com.br; mariaeduarda_ribeiro@outlook.com

RESUMO - Em hidrogeologia, a maioria dos estudos utilizando interpoladores buscam estimar os níveis do lençol freático, as concentrações de contaminantes e a vulnerabilidade de aquíferos. O objetivo principal desta pesquisa foi avaliar qual interpolador geoespacial melhor se adapta a cada um dos seis parâmetros hidrogeológicos selecionados, usando nove testes de consistência. Poços tubulares foram selecionados em uma porção do Sistema Aquífero Fraturado Serra Geral, no Sul do Brasil. Este artigo testou os métodos de Distância Inversa Ponderada, Função de Base Radial, Krigagem Ordinária, Krigagem Lognormal e Cokrigagem. Os resultados apontaram que a Distância Inversa Ponderada apresentou melhor desempenho para os seguintes parâmetros: superfície potenciométrica, primeira zona de fluxo de fratura e segunda zona de fluxo de fratura. A vazão, a transmissividade, a capacidade específica e o nível estático apresentaram baixos níveis de consistência, aumentando consideravelmente as incertezas associadas aos modelos matemáticos para tais parâmetros. Os interpoladores determinísticos superaram os interpoladores estocásticos nas estimativas de parâmetros que apresentaram forte dependência espacial e associação com a litoestratigrafia e a geomorfologia. Esta pesquisa pode contribuir para futuros trabalhos de gestão e planejamento de águas subterrâneas em aquíferos fraturados, uma vez que não foi encontrado na literatura o uso de diferentes métodos de interpolação e índices de consistência para analisar e comparar diversos parâmetros hidrogeológicos em um sistema aquífero fraturado.
Palavras-chave: Interpoladores determinísticos e estocásticos. Parâmetros hidrogeológicos. Águas subterrâneas.

ABSTRACT - In hydrogeology, most studies using interpolators seek to estimate water table elevations, contaminant concentrations and aquifer vulnerability. The primary goal of this research was to evaluate which geospatial interpolator best suits six distinct hydrogeological parameters using nine consistency tests. Water wells were selected on a portion of the Serra Geral Fractured Aquifer System in Southern Brazil. This paper tested the Inverse Distance Weighted, Radial Basis Function, Ordinary kriging, Lognormal kriging and Cokriging methods. The results pointed out that the Inverse Distance Weighted showed better performance for the following parameters: potentiometric surface, first fracture flow zone and second fracture flow zone. Discharge, transmissivity, specific capacity and static level showed low consistency levels, greatly increasing the uncertainties associated with mathematical models for such parameters. Deterministic interpolators surpassed the stochastic interpolators in parameter estimates that presented strong spatial dependence and associations with lithostratigraphy and geomorphology. This research can contribute to future work on groundwater management and planning in fractured aquifers, since the use of different interpolation and consistency approaches to analyze and compare different hydrogeological parameters in a fractured aquifer system has not been found in the literature.
Keywords: Deterministic and stochastic interpolators. Hydrogeological parameters. Groundwater.

INTRODUCTION

The efficient planning and management of groundwater uses depends upon the degree of knowledge of the aquifer. One can reach a better comprehension of the groundwater system through the spatialization of some hydraulic parameters using deterministic and stochastic methods related to the geospatial interpolation. However, the quality of an interpolation varies directly with the knowledge of the sampled points and the interpolator used (Aronoff, 1989).

Interpolators are mathematical tools that assign relative values to a certain variable, building a new dataset, thus converting a range of known discrete data into a continuous one (Castro et al., 2010). Deterministic models (such as the Inverse Distance Weighting and the Radial Basis Function) are based on purely geometric criteria in which the distances are Euclidean, avoiding uncertain measures, while stochastic methods (such as kriging) provide values that are originated from random processes, and are able to quantify the uncertainty associated with the estimator (Yamamoto & Landim, 2013).

Several studies involving evaluation of the best interpolator have been carried out in different fields of science (Belladona & Vargas, 2017; Hernandez-Stefanoni & Ponce-Hernandez, 2006; Kisaka et al., 2016; Mendes & Ribeiro, 2010; Meng et al., 2013; Özdamar et al., 1999; Razack & Lasm, 2005; Sajid et al., 2013; Saraiva et al., 2017; Tadić et al., 2015; Vargas et al., 2018). In hydrogeology, nonetheless, the evaluation of interpolators is not common and no more than a handful of studies was found in the literature.

Delbari (2014) compared different interpolators for predicting the water level of an unconfined sedimentary aquifer (Iran), while Yao et al. (2014) estimated the decline in the water table level in the Wuwei Oasis sedimentary aquifer (China), and both studies found that stochastic methods provide more accurate estimates than deterministic models. Adhikary & Dash (2017) analyzed the groundwater level variation in fractured and sedimentary aquifers in India, before and after the monsoon season, using different interpolator models. Their research found that the Radial Basis Function method performed better than Ordinary kriging for predicting water levels.

Different interpolators were also used to estimate the geospatial distribution of aquifer transmissivity. Muñoz-Pardo & Garcia (1989) compared kriging combined with linear regression and Cokriging methods to determine the best interpolator for transmissivity data of a sedimentary aquifer in Santiago Valley, Chile. Their study identified the first method as the best estimator. Another study regarding interpolating transmissivity values was conducted by Al-Murad et al. (2018), in Kuwait, where Ordinary kriging was defined as the most appropriate to estimate the spatial distribution of transmissivity in sedimentary and karstic aquifers studied.

In Brazil, for instance, mathematical interpolation has helped quantifying aquifer vulnerability (Gomes et al., 2021), groundwater modelling boundary conditions (Silva et al., 2013) and establishing the potentiometric surface (Nobre et al., 2009; Borges et al., 2017; Vargas et al., 2018), but no comparison amongst the interpolators or uncertainty check has been performed in fractured aquifer, only in sedimentary aquifer (Hernandez et al., 2020).

Despite these few studies, a more rigorous consistency testing is still needed in the study of the hydrogeology of fractured aquifers, especially of volcanic rock. A lack in the literature for the interpolation of the fracture flow zones and the specific capacity was also observed.

In order to address these knowledge gaps, this study made use of geostatistics based upon deterministic and stochastic methodologies approaches in the Serra Geral Fractured Aquifer System. This research aims to determine whether geospatial mathematical models are applicable to the analysis of the Fracture Flow Zones and the Specific Capacity parameters. As a second objective, it checks if such models suit the following hydrogeological parameters: Potentiometric Surface, Static Level, Discharge and Transmissivity. Finally, to test the interpolators' consistency, this study use nine consistency analysis methods: Cross validation (Root mean square error), Nash-Sutcliffe, Pearson correlation coefficient, Coefficient of determination, Confidence or performance index, Concordance index, Mean bias, Mean absolute error and D$_{\text{PIELKE}}$.

MATERIAL AND METHODS

Study Area

In the southern Brazil, more especifically in Rio Grande do Sul State, the climate is classified, based on Köppen's, as Subtropical (Cfa) and Temperate (Cfb). During the summer temperature can reach 37°C, while in the winter it can drop to -2°C (Becker et al., 2020). This study evaluated an area in the Rio Grande do Sul state, within the Guaíba Hydrographic Region. The area is situated within the Caxias do Sul Metropolitan Region (CSMR) covering, depending on the hydrogeological parameter investigated, a range between 2,148 and 11,251 km² (Figure 1). The region is very humid, with an average annual

temperature between 14°C and 17.2°C (Rossato, 2011) and the rainfall ranges from 1,750 to 2,400 mm·year^{-1} (Belladona & Vargas, 2017). According to Köppen's climate classification, the area of study is classified as Temperate (Cfb) (Pidwirny, 2006). The municipality of Caxias do Sul sits on the Planalto das Araucárias Geomorphologic Region (IBGE, 1986), where the topography varies between 30 and 1,000 m above mean sea level (Belladona & Vargas, 2017).
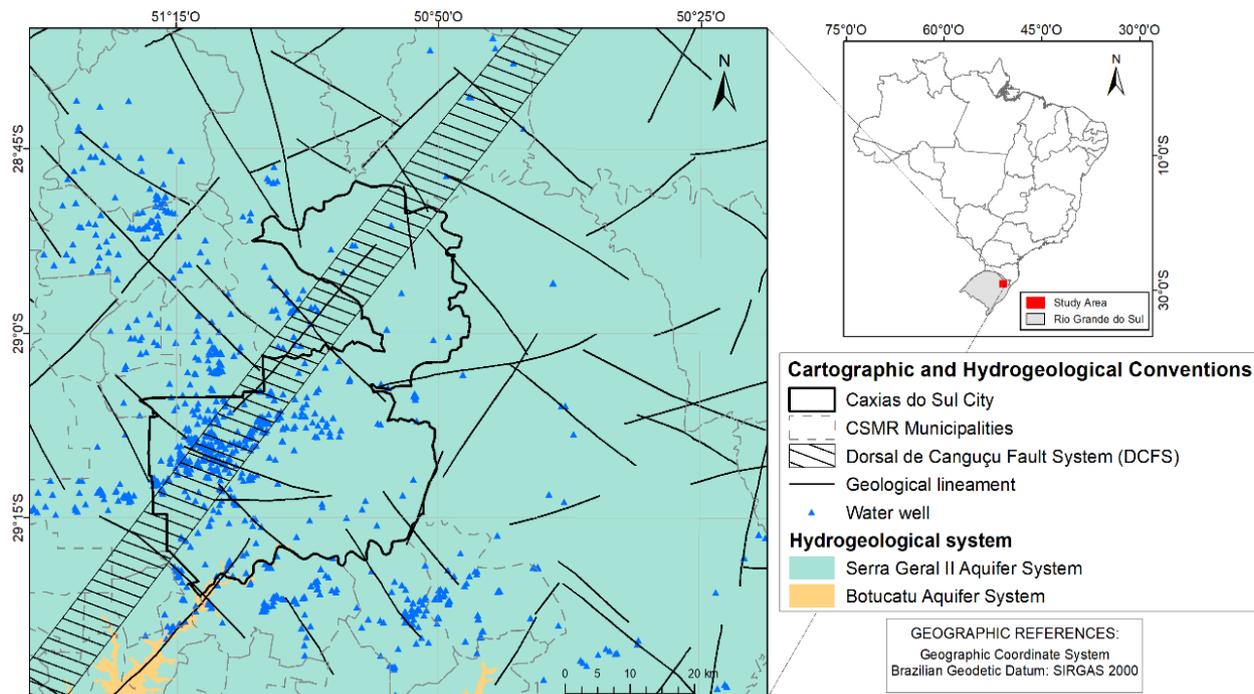
Figure 1 - Location of study area. Hydrogeological setting and water wells set of the assessed areas is also shown.

Geological Background

The south of Brazil presents a diversified geology, comprising geological eras from the Neoarchean to the recent Cenozoic. The investigated site is within the intracratonic basin of Paraná Province that holds the São Bento Group. This group is composed of Guará, Botucatu and Serra Geral Formations, originating from continental environments and volcanic eruptives related to the opening of the South Atlantic. Serra Geral Formation in Brazil is mostly composed of tholeiitic basalts with minor rhyolites and rhyodacites in the upper portion (Melfi et al., 1988).

In southern Brazil, Serra Geral Formation lithologies constitute the volcanic package that are represented by basalts (Gramado Facies), at the base of the sequence, while in the upper portion, rhyodacites, rhyolites, and dacites from the Palmas and Chapecó Facies are identified (Roisenberg & Viero, 2000) and vitrophyres from the Várzea do Cedro Facies (CPRM, 2011). Roisenberg & Viero (2000), through lithostratigraphic profiles (E-W e N-S), demonstrated that the basic and acidic volcanic packages are found in higher elevations in the eastern and northern regions and in lower altitudes in the western and southern areas. Such tendency of altitude reduction of the volcanic package is confirmed by the Paraná basin geomorphology, in the Planalto das Araucárias geomorphological class, situated in the south of Brazil. Planalto das Araucárias has a predominant east to west/southwest deep direction (Almeida, 1956) and in the area of study it is south/southwest (Lisboa et al., 2003). In the Caxias do Sul municipality region, there is a predominance of acidic volcanic flow outcrops of the Serra Geral Formation, while, in a subordinate form, basalt exposures and the Botucatu Formation are observed (Vargas et al., 2013).

The NE-SW lineaments are predominant in the study area, with the NW-SE and E-W lineaments being less expressive (Betiollo, 2006). The geological fault that crosses the city limits (Caxias Fault) has a general direction of N30E, an approximate length of 70 km and a slip of about 100 m between the lowered western block to the uplifted eastern one (Lisboa et al., 2003). The structural geology of the Caxias Fault is related to the geological model of the Dorsal de Canguçu Fault System (DCFS). The DCFS is formed by strike slip faults NE-SW (Figure 1). It is one of the dominant fault systems in the Escudo Sul-riograndense geotectonics region (Picada, 1971).

Hydrogeological Background

In a regional scale, SGAS covers the southeast and south portions of Brazil, belonging to the Paraná Basin geology and covering an area of approximately 917,000 km^2, with a volume of more than 600,000 km^3 (Frank et al., 2009; Fernandes et al., 2016). Fernandes et al. (2016) explain that the contact zones of the different volcanic flows are the main paths to water flow, emphasizing that in the basaltic rocks of the Serra Geral Formation the sub-horizontal fractures with the longest extents are the ones with higher water transmissivity. Therefore, the lithostratigraphy of the volcanic packages influences the horizontal groundwater direction that flows among the contacts and the vesicular and amygdaloid zones (Reginato, 2003).

CPRM (2019) classifies the fractured aquifer of the Serra Geral Formation in the area of study as the Serra Geral II Aquifer System (SGAS II), Figure 1. Machado & Freitas (2005) note that the SGAS II characterizes the hydrogeology of the region, where volcanic rocks of acidic to intermediate composition are predominant. The specific capacity is in general lower than 0.5 m^3·h^{-1}·m^{-1}, nonetheless, in intense fractured regions or at sites where sandstone ocurrs at the base of the system, this value can be as high as 2 m^3·h^{-1}·m^{-1} (CPRM, 2019).

In the northeast region of Rio Grande do Sul, where SASG II is found, Reginato & Strieder (2006) identified a predominance of water wells with discharge rates above 20 m^3·h^{-1} in the N10-14S, N20-30E, N40-50E, N30-40W, N50-60W, and N80-90W lineament directions. Throughout the Caxias do Sul Metropolitan Region, water wells in the SGAS II present discharge rates 71% below 10 m^3·h^{-1}, 18% between 10 and 20 m^3·h^{-1} and 11% above 20 m^3·h^{-1}; static water level depths varied from 0 to 10 m for 36% of observed water wells, while 25% is between 10 and 20 m, and 39% greater than 20 m (Vargas et al., 2018).

Hydrogeology dataset

The technical terminology used in this study is as follows: Potentiometric Surface, Static Level, Discharge, Transmissivity and Specific Capacity, following the hydrogeological glossary of the Brazilian Geological Service (CPRM, 2020). CPRM (2020) explains that the Potentiometric Surface is the mechanical energy level of the water in a water well. In the Serra Geral Fractured Aquifer System, such a surface show a similar behavior to the piezometric surface observed in confined aquifers (De Vargas et al., 2021).

The Static Level represents the water level in a water well, which is not necessarily the water table. 1st Fracture Flow Zone and 2nd Fracture Flow Zone parameters represent the first and the second fractures that allow water flow into the studied water wells. Potentiometric Surface, 1st Fracture Flow Zone and 2nd Fracture Flow Zone parameters have altimetric elevation in relation to mean sea level, while Static Level is measured in relation to ground surface. Potentiometric Surface, Static Level, 1st Fracture Flow Zone and 2nd Fracture Flow Zone, Discharge, Transmissivity and Specific Capacity datasets come from water wells (Figure 1) selected from the Public Water and Wastewater Service (SAMAE) of the city of Caxias do Sul and from the Groundwater Information System (SIAGAS) of the Brazilian Geological Service (CPRM, 2018).

The selected water wells were those that fulfilled the requirements of design, construction and hydrodynamic testing established by the Brazilian technical standards (ABNT, 2006a, b) and that extracts water from the fractured rock. Table 1 shows the number of water wells used and their density per square kilometer for the study area.

Table 1 - Quantity of water wells used for each parameter and the respective water well density per km^2.

Parameter	N^o of water wells	Total area (km^2)	Water well·km^{-2}
Potentiometric Surface	884	11,251	0.08
Static Level	884	11,251	0.08
1st Fracture Flow Zone	269	6,309	0.04
2nd Fracture Flow Zone	147	2,148	0.07
Discharge	926	11,251	0.08
Transmissivity	127	3,317	0.04
Specific Capacity	552	10,989	0.05

Interpolator Methods

The interpolators used in this study were the Inverse Distance Weighting (IDW), the Radial Basis Function completely regularized spline type (RBF-R) and the spline with tension type (RBF-T), Ordinary kriging (OK), Lognormal

kriging (LK) and Cokriging (CK). Interpolators were handled in ESRI's ArcGIS 10.4.1 software and used minimum and maximum numbers of neighbors equal to 2 and 5, respectively.

The IDW method predicts the value for an unsampled point using the values sampled around it (Jakob & Young, 2006). It gives weight to data points such that their influence on prediction is reduced as distance from the point increases (Landim, 2000). Mathematically, it can be described by considering Z as the interpolated value, Z_i is the ith data value, h_{ij} denotes the separation distance between interpolated value and the sample data value, and β denotes the weighting power while n represents the total number of sample data values (Equation 1):

$$Z = \frac{\sum_{i=1}^{n} \frac{z_i}{h_{ij}^{\beta}}}{\sum_{i=1}^{n} \frac{1}{h_{ij}^{\beta}}} \qquad (1)$$

The RBF-R and RBF-T methods use polynomials to fit a surface with the minimum curvature passing through all samples, resulting in a smoothed surface (Landim, 2000). These methods represent a real function where the value depends on the distance from the origin (Adhikary & Dash, 2017) and derivation calculations are performed until a tolerance between the sampled and estimated values, or a maximum number of interactions, is reached (Landim, 2000). The RBF-R and RBF-T methods can be demonstrated by $\Phi(X) = \Phi(\|X\|)$ and the norm is usually Euclidean distance, although other distance functions are also possible (Adhikary & Dash, 2017).

Kriging is a geostatistical method that takes into account the spatial characteristics of the autocorrelation of the regionalized variables, in which there must be spatial continuity, allowing the data obtained by sampling to be used to parameterize the estimation of points where there is no information (Landim, 2000). It is an exact interpolator that takes into account all observed values, with the best-known algorithm being OK. Mathematically, it can be described by considering $\hat{Z}(x_0)$ as the kriging estimate at location x_0, $Z(x_i)$ is the sampled value at x_i and λ_i is the weighing factor associated with $Z(x_i)$ (Equation 2):

$$\hat{Z}(x_0) = \sum_{i=1}^{n} \lambda_i Z(x_i) \qquad (2)$$

On the other hand, LK is best applied for interpolating data that present a positive skewness histogram, thus ensuring that the distribution of the transformed values is normal (Yamamoto & Landim, 2013). In this research, the natural logarithmic transformation was performed whenever data presented a positive skewness histogram.

CK is a multivariate extension of the kriging method that uses two or more variables to improve the estimative of the primary variable. CK can only be considered relevant when the primary variable has a considerably reduced number of cases in relation to the secondary variable (Yamamoto & Landim, 2013).

Consistency analysis methods

Interpolation methods were evaluated by Cross Validation with the leave-one-out technique, which allowed analyzing the efficiency estimation of interpolated models using the Nash-Sutcliffe efficiency (*NSE*), Pearson correlation coefficient (*r*), Coefficient of determination (r^2), Confidence or performance index (*c*), Concordance index (*d*), Mean bias (*MB*), Mean absolute error (*MAE*), Root mean square error (*RMSE*) and D_{PIELKE} methodologies. The leave-one-out cross validation method is explained in more detail in Syed (2011). Further reading on the consistency methodology equations can be found in the following citations: Pearson's Correlation coefficient can be determined as r = Strong (0.7 to 1), Moderate (0.4 to 0.6) and Weak (0.1 to 0.3), being the equation defined in Dancey & Reidy (2006). The c proposed by Camargo & Sentelhas (1996) was established as Great ($c > 0.85$), Very Good ($0.76 \leq c \leq 0.85$), Good ($0.66 \leq c \leq 0.75$), Median ($0.61 \leq c \leq 0.65$), Regular ($0.51 \leq c \leq 0.60$), Bad ($0.41 \leq c \leq 0.50$) and Poor ($c \leq 0.40$). This latter index can be obtained by multiplying r and d. The Concordance index is classified within the limits $0 \leq d \leq 1$, being 0 concordance absence and 1 perfect concordance (Willmot, 1982). Another relevant factor is r^2, which is an indicator of the degree to which the regression explains the sum of total square (Gardiman Junior et al., 2012), ranging from 0 to 1, and the closer to 1, the better the model (Saraiva et al., 2017).

Alternatively, the *NSE* method relates the difference between simulated values and observed values, showing a variation in four ranges: Very Good for $0.75 < \text{Nash} \leq 1$; Good for $0.65 < \text{Nash} \leq 0.75$; Satisfactory for $0.5 < \text{Nash} \leq 0.65$; and Unsatisfactory for values equal to or less than 0.5 (Moriasi et al., 2007).

The *MB* analysis indicates the model tendency to overestimate or underestimate the predicted value in relation to what was observed, while the *MAE* method can be considered accurate and robust for use in numerical models (Hallak & Pereira Filho, 2011). The lower the *MAE* value, the closer the estimated value will be to the observed one. Another methodology applied to quantify accuracy is *RMSE*, which shows a similar rationality to Mean Square Error. However, Hallak & Pereira Filho, (2011) show that the *RMSE* presents error values in the same dimensions of the analyzed variable which is an advantage. According to Al-Murad et al. (2018), the *RMSE*

must be less than 10% of the range (between the minimum and maximum) of the observed parameter value, e.g. Potentiometric Surface. An additional index (D_{PIELKE}), proposed by Pielke (2002), can evaluate the numerical model dexterity regarding simulation quality. It is observed that: a) dexterity can be demonstrated when $D_{PIELKE} <$ 2; b) in a set of several simulations of the same case, the smallest D_{PIELKE} is the best simulation; c) a perfect simulation is considered when $D_{PIELKE} = 0$ (Hallak & Pereira Filho, 2011).

In order to aid the reader, Figure 2 depicts a detailed flowchart of the framework used in this study.
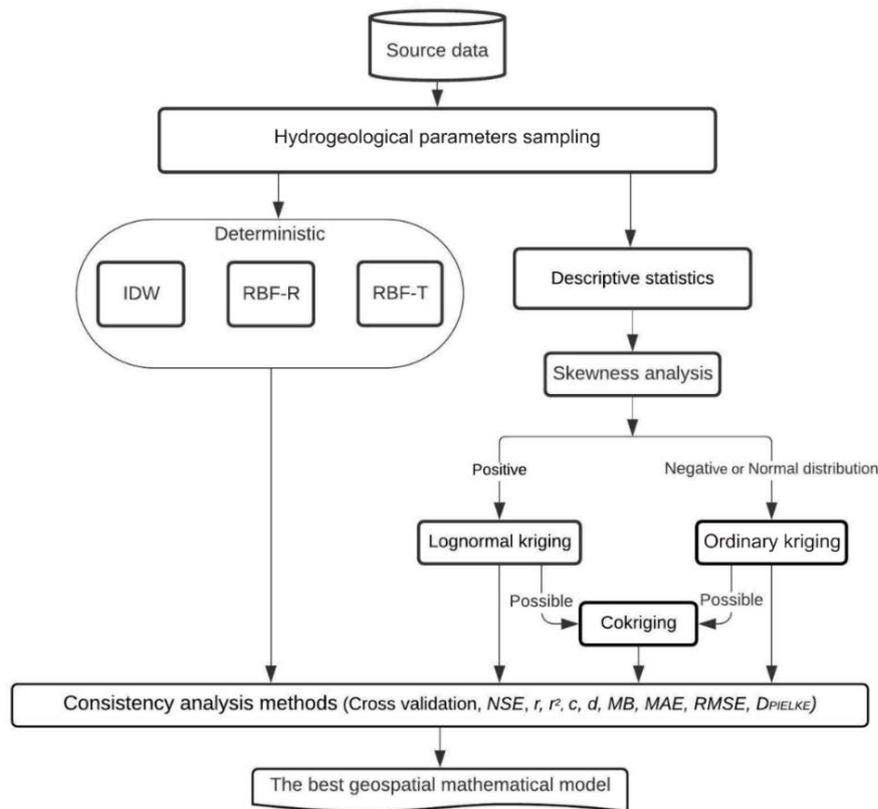
Figure 2 - Flowchart summarizing the methodology adopted in this study.

RESULTS AND DISCUSSION

Statistical analysis

The descriptive statistical analysis shows high standard deviation (σ) values for Potentiometric Surface, Static Level, 1st Fracture Flow Zone and 2nd Fracture Flow Zone, explained by the wide range between their minimum and maximum values.

For instance, the Potentiometric Surface varies from 6.1 to 1,001.5 meters (Table 2). In addition, the high values identified for Discharge, Transmissivity and Specific Capacity also shows a wide range between the minimum and maximum values (Table 2). This behavior is

typical of fractured aquifer systems, which do not present constant hydrodynamic parameters due to strong heterogeneity and anisotropy (Reginato, 2003; Reginato & Strieder, 2006; Fiume et al., 2020). All parameters evaluated revealed histograms with leptokurtic kurtosis. In addition, Static Level, Discharge, Transmissivity and Specific Capacity showed positive skewness. When inappropriate to use positive skewness variables in kriging, the logarithmic transformation (Yamamoto & Landim, 2013) was applied to obtain a normal distribution or a negative skewness (Table 2).

Table 2. Statistical description and skewness values observed in Potentiometric Surface, Static Level, 1st Fracture Flow Zone, 2nd Fracture Flow Zone, Discharge, Transmissivity and Specific Capacity, and skewness and kurtosis values after logarithmic transformation.

Parameter	Min	Max	Mean	SD	Skewness	Kurtosis	Logarithmic transformation	
							Skewness	Kurtosis
Potentiometric Surface (m)	6.10	1,001.5	651.7	185.7	-1.89	6.68	NTR	NTR
Static Level (m)	0.05	162.1	23.6	25.2	1.98	7.67	-0.694	3.757
1st Fracture Flow Zone (m)	10.0	860.0	657.0	113.1	-2.07	11.59	NTR	NTR
2nd Fracture Flow Zone (m)	64.0	826.7	624.6	101.3	-1.77	9.83	NTR	NTR
Discharge (m³·h⁻¹)	0.10	67.1	8.7	9.3	2.50	10.84	-0.357	3.452
Transmissivity (m²·h⁻¹)	0.001	47.6	2.24	6.12	4.90	30.61	-0.029	2.460
Specific Capacity (m³·h⁻¹·m⁻¹)	0.001	14.4	0.88	1.76	4.11	23.48	-0.209	2.658

NTR: No Transformation Required

The spatial dependence or randomness of the observed parameters was analyzed through the ratio between the nugget and sill, which can be classified according to Liu et al. (2006) and Guerra (1988), Table 3. The semivariograms developed through the OK and the LK methods established low nugget and sill values for all variables analyzed in the study area (Table 4).

Table 3 - Classification based on the nugget-sill ratio.

Spatial Dependence (D). Liu et al. (2006).	Degree of Randomness (E). Guerra (1988).
Strong: D ≤ 0.25	Small: E < 0.15
Moderate: 0.25 ≤ D ≤ 0.75	Significant: 0.15 ≤ E ≤ 0.30
Weak: D > 0.75	Very significant: E > 0.30

Table 4 - Values obtained in semivariograms and ratio between nugget and sill to classification of spatial dependence or randomness.

Parameter	Nugget	Sill	Range (m)	Nugget/Sill	Classification	
					Liu et al. (2006)	Guerra (1988)
Potentiometric Surface	0.07	0.51	2.98	0.14	Strong	Small
Static Level	1.08	1.68	2.02	0.64	Moderate	Significant
1st Fracture Flow Zone	0.17	2.02	2.41	0.08	Strong	Small
2nd Fracture Flow Zone	0.07	1.30	1.91	0.06	Strong	Small
Discharge	0.19	1.02	5.99	0.18	Strong	Significant
Transmissivity	0.34	0.58	4.92	0.59	Moderate	Very significant
Specific Capacity	0.00	0.25	2.53	0.00	NC	NC

NC: No Classified

Applying the method specified by Liu et al. (2006), strong spatial dependence was found in all parameters evaluated except for Static Level and Transmissivity that showed a moderate dependence level. However, the method proposed by Guerra (1988) points out a significant degree of randomness to Discharge, a very significant degree of randomness to Static Level and Transmissivity and a small degree of randomness to Potentiometric Surface, 1st Fracture Flow Zone and 2nd Fracture Flow Zone (Table 4).

In both applied methodologies, Potentiometric Surface, 1st Fracture Flow Zone and 2nd Fracture Flow Zone showed strong spatial dependence (small degree of randomness), while a less influence of spatial dependence was observed in Discharge and Transmissivity. This low spatial dependence is related to the heterogeneity and anisotropy of the SGAS II. Conversely, Static Level showed a high degree of randomness, while Specific Capacity could not be evaluated due to the nugget value (0.00), Table 4. The high randomness attributed to the Static Level is probably due to the ground surface oscillation in relation to the Static Level of the water well in the local scale, while the strong spatial dependence on Potentiometric Surface, 1st Fracture Flow Zone and 2nd Fracture Flow Zone is linked to the regional lithostratigraphic and geomorphological behavior described by Almeida (1956), Roisenberg & Viero (2000), Lisboa et al. (2003) and Reginato (2003).

Interpolated hydrogeological parameter analysis

The efficiency of the interpolators was tested and compared for all hydrogeological parameters listed in this study.

Potentiometric Surface, 1st and 2nd Fracture Flow Zones

Potentiometric Surface showed r, c and *NSE* with maximum and identical values (Strong, Great and Very Good) in all interpolators, whereas the d, r^2, *MAE* and *RMSE* exposed more favorable values to the IDW method (Table 5). In this case, it was possible to observe the best d (0.981) and the smallest *RMSE* (50.00). The remainder *RMSE* values are within the 10% limit value (99.5 m) identified between the minimum and maximum. The IDW method also showed greater dexterity with D_{PIELKE} close to 2 (2.009), thus confirming the best interpolation performance. The favorability order of this parameter was identified as IDW > OK > RBF-T > RBF-R.

Interpolators applied to 1st Fracture Flow Zone were classified by r as Strong, by c as Good and by *NSE* as Good (Table 5). However, the D_{PIELKE} index showed dexterity values above 2. The best interpolator method was the IDW, which presented $d = 0.894$ and *RMSE* = 63.59. The remainder *RMSE* values are within the 10% limit value (85 m) identified between the minimum and maximum values. The favorability order of this parameter was identified as IDW > RBF-T > RBF-R > OK. In order to improve the results of 1st Fracture Flow Zone (269 water wells), the CK interpolator was applied using the Discharge parameter (926 water wells), however, this interpolator did not obtain better performance than the IDW (Table 5). Most consistency indexes presented satisfactory results for 1st Fracture Flow Zone, thus validating the geospatial mathematical models. In addition, the performance order of the interpolators was quite similar to the one observed in the Potentiometric Surface.

Table 5 - Consistency index values for Potentiometric Surface, 1st Fracture Flow Zone and 2nd Fracture Flow Zone using IDW, RBF-R, RBF-T, OK and CK interpolators.

Index	r	d	r²	c	NSE	MB	MAE	RMSE	D_PIELKE
Potentiometric Surface									
IDW	0.96	0.981	0.928	0.94	0.93	2.32	30.29	50.00	2.009
RBF-R	0.96	0.976	0.914	0.93	0.91	0.14	33.95	54.66	2.033
RBF-T	0.96	0.978	0.918	0.94	0.92	1.48	33.06	53.14	2.024
OK	0.96	0.979	0.922	0.94	0.92	0.43	32.65	51.99	2.016
1st Fracture Flow Zone									
IDW	0.83	0.894	0.686	0.74	0.68	4.30	42.05	63.59	2.209
RBF-R	0.82	0.888	0.674	0.73	0.67	1.75	43.40	64.71	2.222
RBF-T	0.83	0.896	0.681	0.74	0.68	2.70	44.08	63.84	2.207
OK	0.81	0.891	0.664	0.73	0.66	0.05	43.18	65.43	2.224
CK	0.82	0.892	0.665	0.73	0.66	0.02	43.17	65.37	2.223
2nd Fracture Flow Zone									
IDW	0.78	0.858	0.602	0.67	0.60	3.28	38.45	63.81	2.247
RBF-R	0.76	0.841	0.581	0.64	0.58	0.85	39.38	65.55	2.274
RBF-T	0.77	0.848	0.587	0.65	0.59	1.03	38.96	65.01	2.259
OK	0.77	0.862	0.600	0.67	0.60	0.69	41.77	63.89	2.260

The 2nd Fracture Flow Zone parameter also revealed the IDW ($d = 0.858$; *RMSE* = 63.81) as the best interpolator method. The remainder *RMSE* values are within the 10% limit value (76.3 m) identified between the minimum and maximum. The interpolators were classified by r as Strong, by c as Good to Median, and by *NSE* as Satisfactory (Table 5). However, the D_{PIELKE} index showed dexterity values above 2. For 2nd Fracture Flow Zone, the interpolators favorability order was IDW > OK > RBF-T > RBF-R. Therefore, similar to 1st Fracture Flow Zone, this parameter showed satisfactory results for valida-ting the applied geospatial mathematical models. The performance order of the interpolators was very similar to that observed in 1st Fracture Flow Zone and Potentiometric Surface.

Regarding the *MB* for Potentiometric Surface, 1st Fracture Flow Zone and 2nd Fracture Flow Zone, it can be observed that all interpolators tested showed positive *MB*, some of which were close to zero which reflects overestimated estimates of the generated models.

For Potentiometric Surface, 1st Fracture Flow Zone and 2nd Fracture Flow Zone the IDW deterministic method proved to be more appro-

priate. Landim (2000) asserts that IDW shows an efficient performance to obtain digital terrain models, presenting a good relationship with the topography. These singularities contribute to the understanding of performance results, since in the study area there are areas with deep valleys with cliffs. This interpretation is supported by the classification of a high spatial dependence and by a reduction in altimetry towards the south,

southwest and west on Potentiometric Surface, 1st Fracture Flow Zone (Figure 3) and 2nd Fracture Flow Zone, similar to the tendency observed in the geomorphology and lithostratigraphy of volcanic flows in the region (Almeida, 1956; Roisenberg & Viero, 2000; Lisboa et al., 2003; Reginato, 2003). Therefore, the geological characteristics of the area must be given the due importance in order to assess an appropriate interpolator.
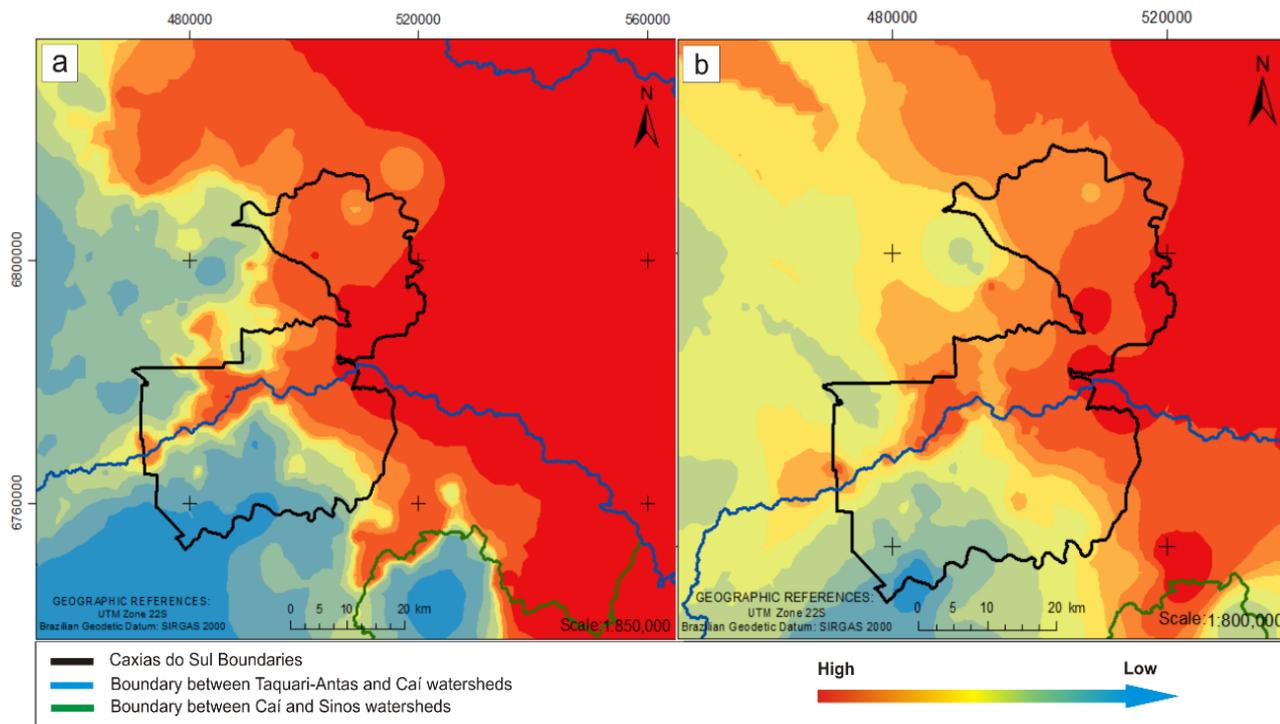
Figure 3 - IDW geospacial model. (a) Potentiometric Surface and (b) 1st Fracture Flow Zone.

Static Level, Discharge, Transmissivity and Specific Capacity

Static Level demonstrated r, r^2, c and *NSE* with low values in all tested interpolators. Although Static Level showed apparently low *RMSEs*, this index exceeded the limit of 10% (16.2 m) between the minimum and maximum values. In addition, d reached intermediate values and D_{PIELKE} showed dexterity values considerably above 2, thus demonstrating low efficiency in all interpolation methods applied (Table 6). Therefore, the RBF-T interpolator was chosen to represent the low efficiency identified in the geospatial mathematical modeling (Figure 4a - measured vs predicted correlation graph).

All interpolators presented low efficiency values (r, d, r^2, c and *NSE*) for Discharge, being classified by r from Moderate to Weak, by c as Poor and by *NSE* as Unsatisfactory. In addition, they showed D_{PIELKE} values above 2 and *RMSE* values above 10% (6.7 m^3·h^{-1}) of the range between the minimum and maximum values.

Considering the indexes r, d, r^2, c, *NSE*, D_{PIELKE} and *RMSE*, all interpolation methods can be classified as inconsistent (Table 6). To represent the inconsistencies observed in the geospatial mathematical models obtained for Discharge. It is possible to view the correlation graph produced by LK in the Figure 4b.

Transmissivity and Specific Capacity showed inconsistency values in the r, d, r^2, c, *NSE*, D_{PIELKE} and *RMSE* indexes, similar to what was observed for Discharge. Both Transmissivity and Specific Capacity were classified by r as Weak, by c as Poor and by *NSE* as Unsatisfactory (Table 6). D_{PIELKE} showed values higher than 2, while *RMSE* showed quantitative above 10% (Transmissivity: 4.76 m^2·h^{-1} and Specific Capacity: 1.44 m^3·h^{-1}·m^{-1}) of the range between the minimum and maximum value. Based on these results, all interpolators tested for Transmissivity and Specific Capacity are inadequate. The low efficiency identified in the geospatial modeling, by the consistency indices, performed for the

Specific Capacity is corroborated by the low correlation of the data in the predicted vs. measured correlation graph. The RBF-R interpolator correlation plot (Figure 4c) was selected to graphically represent the low correlation observed in all interpolations.

The CK method was applied to Transmissivity (127 water wells) with the aid of Specific Capacity (552 water wells), in search for an improvement of Transmissivity results. However, the results obtained for c and NSE were not significantly improved from those obtained previously for Transmissivity, but r changed from Weak to Moderate, d and r^2 increased considerably which D_{PIELKE} decreased (Table 6). Nevertheless, $RMSE$ remained above 10% (4.76 $m^2 \cdot h^{-1}$). Notwithstanding, the interpolations using CK continued with a high degree of inconsistency, although they showed better results than other interpolators did. The graph showing the low correlation between predicted vs. measured data for CK is shown in figure 4d.
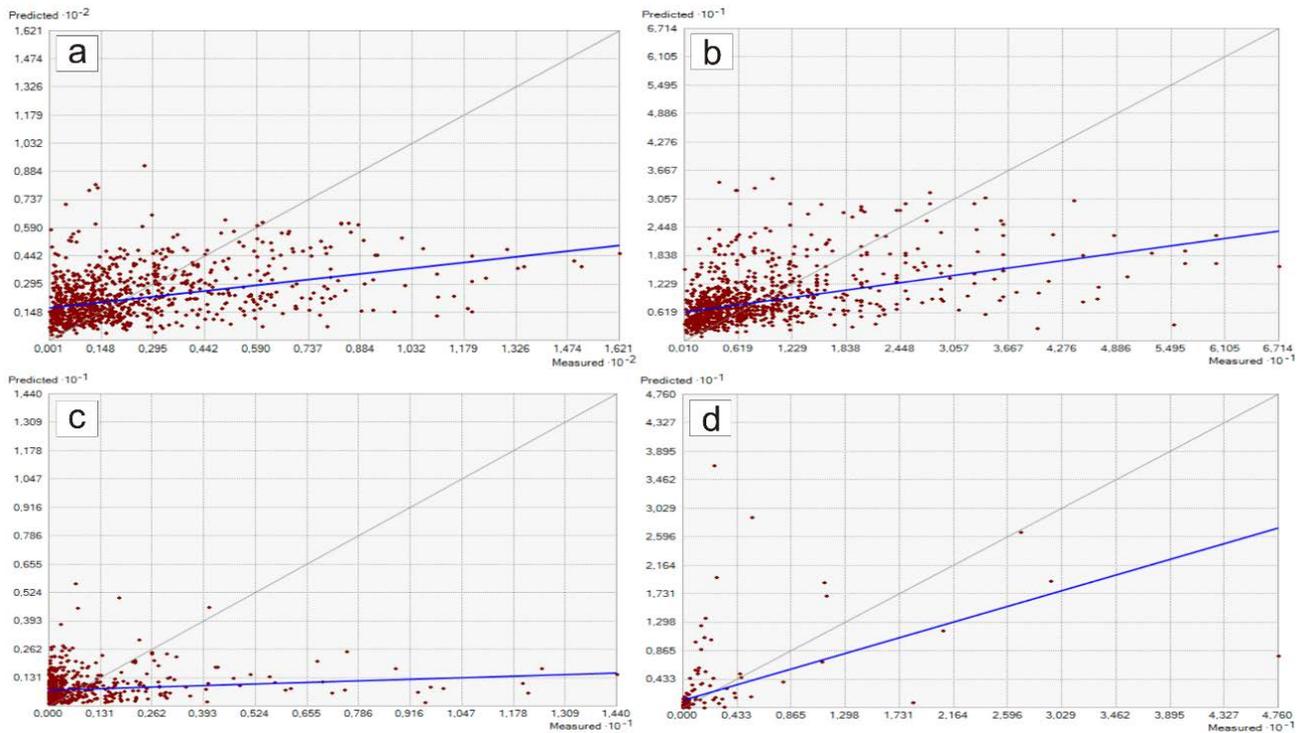
Figure 4 - Correlation graphs of measured *vs.* predicted values to (a) Static Level, (b) Discharge, (c) Specific Capacity and (d) Transmissivity.

The Static Level showed negative *MB* (underestimated model) and close to zero for the evaluated interpolators, except for the LK interpolator. Regarding the *MB* for Discharge, Specific Capacity and Transmissivity the interpolators tested for Discharge showed positive *MB*, indicating overestimated modeling. RBF interpolators for Specific Capacity showed equal to zero and close to zero *MB*. On the other hand, Transmissivity showed negative *MB* (underestimated model) and close to zero for deterministic interpolators, while the stochastic interpolators resulted in an overestimated model (Table 6).

The modeling performed for Static Level, Discharge, Transmissivity and Specific Capacity did not define which geospatial interpolator was most adequate, although some interpolators were presented with subtly higher efficiency indexes than others.

This lack of definition occurred due to the low values of efficiency indexes, leading to high estimate inconsistency. The lack of data consistency is probably associated with poor homogeneity and strong anisotropy of the environment. The anisotropy of the studied aquifer was verified by the low spatial dependence presented by Static Level, Discharge, Transmissivity and Specific Capacity, and by the great variability of the Transmissivity and Specific Capacity values. However, the CK interpolator showed an improvement in the efficiency indexes in relation to other interpolators used for Transmissivity. Thus, CK presents a better performance trend in a heterogeneous and anisotropic environment of the fractured aquifer, considering a regional extension.

Table 6 - Consistency index values of Static Level, Discharge, Transmissivity and Specific Capacity, using IDW, RBF-R, RBF-T, LK and CK interpolators.

Index	r	d	r^2	c	NSE	MB	MAE	RMSE	D_{PIELKE}
Static Level									
IDW	0.33	0.555	0.110	0.18	-0.01	-0.33	16.57	25.28	2.470
RBF-R	0.36	0.543	0.128	0.19	0.09	-0.09	16.29	24.03	2.481
RBF-T	0.38	0.545	0.141	0.20	0.12	-0.01	16.19	23.62	2.481
LK	0.35	0.541	0.124	0.19	0.07	2.79	17.62	24.26	2.504
Discharge									
IDW	0.41	0.607	0.167	0.25	0.07	0.09	5.62	9.04	2.369
RBF-R	0.34	0.562	0.117	0.19	-0.09	0.23	6.01	9.77	2.426
RBF-T	0.44	0.596	0.191	0.26	0.17	0.03	5.51	8.53	2.384
LK	0.45	0.614	0.202	0.28	0.17	0.54	5.64	8.52	2.360
Transmissivity									
IDW	-0.03	0.137	0.001	0.00	-0.29	-0.25	3.08	6.91	2.764
RBF-R	0.00	0.135	0.000	0.00	-0.15	-0.05	3.11	6.53	2.754
RBF-T	0.01	0.142	0.000	0.00	-0.13	-0.05	3.09	6.47	2.753
LK	0.00	0.166	0.000	0.00	-0.50	1.70	4.39	7.46	2.808
CK	0.47	0.646	0.223	0.30	-0.05	0.82	2.50	6.25	2.220
Specific Capacity									
IDW	0.15	0.345	0.021	0.05	-0.23	0.02	1.03	1.95	2.618
RBF-R	0.15	0.300	0.023	0.05	-0.03	0.00	0.98	1.79	2.673
RBF-T	0.15	0.294	0.023	0.04	-0.03	0.00	0.98	1.78	2.681
LK	0.14	0.322	0.018	0.04	-0.07	0.03	1.01	1.82	2.673

The inconsistencies of geospatial mathematical models observed for Discharge, Transmissivity and Specific Capacity are associated with the heterogeneity and anisotropy of SGAS II. Reginato (2003), studied the Transmissivity and Specific Capacity of 11 regions in SGAS II, and determined the minimum and maximum values between the means obtained in these regions (Transmissivity: from 0.133 to 1.458 $m^2 \cdot h^{-1}$; Specific Capacity: from 0.106 to 1.166 $m^3 \cdot h^{-1} \cdot m^{-1}$), demonstrating that this variability is related to the strong anisotropy of the aquifer systems. In the study area, a large variability in Transmissivity (from 0.001 to 47.6 $m^2 \cdot h^{-1}$) and Specific Capacity (from 0.001 to 14.4 $m^3 \cdot h^{-1} \cdot m^{-1}$) was also observed, thus proving the strong anisotropy in SGAS II. Therefore, the anisotropy of SGAS II influenced the results of the consistency of the evaluated geospatial mathematical models.

CONCLUSION

Most studies involving hydrogeological parameter interpolation indicate kriging as the most appropriate, though this current research found the best approach to be unique for most evaluated hydrogeological parameters in the fractured aquifer of volcanic rock. In the area of study, the parameters that presented a strong spatial dependence which were closely related to the geomorphology and to the lithostratigraphy were best estimated by deterministic rather than stochastic interpolators.

Although the favorability order of the interpolators is different among most of the parameters, the consistency indexes in most cases showed very similar values between deterministic and stochastic models. The performance of the interpolators is linked to the geological and geomorphological complexity of the studied environment site and to the availability of the model input data, as well as to the sampling site distribution and to the model calibration. Therefore, in research on volcanic fractured aquifers that uses geospatial Mathematical models as a basis, it is recommended to perform data consistency checks to different interpolator methods, e.g. aquifer vulnerability analysis applying map algebra or groundwater flow direction determination, that are used in groundwater resource planning and management.

The choice of the most appropriate interpolator has a direct influence on the quality of the final map. In the case of this research, the applied geospatial mathematical models are not adequate to represent the Static Level, the Discharge, the Transmissivity and the Specific Capacity of the fractured aquifer considered. On the other hand, the models used to interpolate Potentiometric Surface, 1st Fracture Flow Zone and 2nd Fracture Flow Zone were considered appropriate to represent the aquifer. This contrast reveals that it is necessary to carry out a consistency analysis of

the interpolators, using different indexes. Static Level interpolations are commonly used in map algebra for aquifer vulnerability classification, while Potentiometric Surface interpolations are applied in determining the groundwater flow direction. Therefore, in volcanic fractured aquifer systems, the Static Level interpolation can represent a significant increase in uncertainties in the definition of aquifer vulnerability, while the interpolation of Potentiometric Surface provides a more reliable result.

This research shows that deterministic geospatial models have fewer uncertainties in the interpolation of hydrogeological parameters that have a strong spatial dependence. On the other hand, the CK stochastic interpolator proved to be an interesting option to manipulate parameter datasets with a high degree of randomness, such as those representing in heterogeneous and anisotropic environments, despite not having obtained adequate indexes. Therefore, this discovery contributes significantly to the field of geostatistics, especially for the production of hydrogeological maps in fractured aquifers of volcanic rock. In addition, this study contributes to hydrogeological science by presenting an innovative comparison and an efficiency testing of a set of parameters (Potentiometric Surface, 1st Fracture Flow Zone, 2nd Fracture Flow Zone, Static Level, Discharge, Transmissivity and Specific Capacity) in a fractured volcanic aquifer system, using different interpolation methods and consistency indexes.

REFERENCES

ABNT (ASSOCIAÇÃO BRASILEIRA DE NORMAS TÉCNICAS). Norma Brasileira 12212: Water well - Procedure for groundwater wells. Rio de Janeiro, Brazil, 2006a.

ABNT (ASSOCIAÇÃO BRASILEIRA DE NORMAS TÉCNICAS). Norma Brasileira 12244: Water well – Construction of groundwater wells. Rio de Janeiro, Brazil, 2006b.

ADHIKARY, P.P. & DASH, C.J. Comparison of deterministic and stochastic methods to predict spatial variation of groundwater depth. Appl Water Sci 7:339–348, 2017. DOI: 10.1007/s13201-014-0249-8.

ALMEIDA, F.F.M. O Planalto Basáltico da Bacia do Paraná. Boletim Paulista de Geografia nº 24, São Paulo, Brasil, 1956.

AL-MURAD, M.; ZUBARI, W.K.; UDDIN, S. Geostatistical characterization of the transmissivity: an example of Kuwait aquifers. Water 10:828, 2018. DOI: 10.3390/w10070828

ARONOFF, S. Geographic information systems: a management perspective. Ottawa, Canada. WDL Publications. 294p, 1989.

BELLADONA, R. & VARGAS, T. Distribuição espaço-temporal das precipitações e a relevância da orografia do município de Caxias do Sul (RS). Revista Brasileira de Cartografia 69(3): 607-620, 2017.

BETIOLLO, L.M. Caracterização estrutural, hidrogeológica e hidroquímica dos Sistemas Aquíferos Guarani e Serra Geral no nordeste do Rio Grande do Sul, Brasil. Master's Thesis - Federal University of Rio Grande do Sul, 2006.

BECKER, C.C.; STRECK, N.A.; UHLMANN, L.O.; SILVEIRA, W.B. Scheduling optimum planting window for gladiola based on El Niño Southern Oscillation. Scientia Agricola, v.77, e20180336, 2020. DOI: https://doi.org/10.1590/1678-992X-2018-0336.

BORGES, V.M.; ATHAYDE, G.B.; REGINATO, P.A.R. Evaluation of natural vulnerability to contamination of Serra Geral aquifer system In Paraná – Brazil. Águas Subterrâneas, v. 31, n. 4, p. 327-337, 2017. DOI: http://dx.doi.org/10.14295/ras.v31i4.28857.

CAMARGO, A.P. & SENTELHAS, P.C. Equação para a estimativa da evapotranspiração potencial no estado de São Paulo, baseada no método de Hargreaves – 1974. Revista Brasileira de Agrometeorologia 4(1):77-81, 1996.

CASTRO, F.S.; PEZZOPANE, J.E.M.; CECILIO, R.A.; PEZZOPANE, J.R.M.; XAVIER, A.C. Avaliação do desempenho dos diferentes métodos de interpoladores para parâmetros do balanço hídrico climatológico. Revista Brasileira de Engenharia Agrícola e Ambiental 14(8):871-880, 2010.

CPRM – BRAZILIAN GEOLOGICAL SURVEY. Projeto Geoparques: Geoparque caminhos dos cânions do sul, 2011. Available via DIALOG. https://www.cprm.gov.br/publique/media/gestao_territorial/geoparques/canions/creditos.html. Accessed 01 September 2021.

CPRM – BRAZILIAN GEOLOGICAL SURVEY. Groundwater Information System. Available via DIALOG. http://siagasweb.cprm.gov.br/layout/index.php. Accessed 02 April 2018.

CPRM – BRAZILIAN GEOLOGICAL SURVEY. Geological base downloads. Available via DIALOG. http://geosgb.cprm.gov.br/geosgb/downloads.html. Acessed 14 August 2019.

CPRM – BRAZILIAN GEOLOGICAL SURVEY. Termos Hidrogeológicos Básicos. Available via DIALOG. http://www.cprm.gov.br/publique/Redes-Institucionais/Rede-de-Bibliotecas---Rede-Ametista/Termos-Hidrogeologicos-Basicos-631.html. Accessed 01 July 2020.

DANCEY, C. & REIDY, J. Estatística sem matemática para psicologia: usando SPSS para Windows. (LV, Trad.). Porto Alegre: Artmed, p.172-180, 2006.

DELBARI, M. Accounting for exhaustive secondary data into the mapping of water table elevation. Arab J Geosci 7:4221-4233, 2014. DOI: 10.1007/s12517-013-0986-2.

DE VARGAS, T., BELLADONA, R., DAL BOSCO, V., & ADAMI, M. V. D. (2021). Serra Geral Fractured Aquifer System: confined or unconfined? 47TH IAH Congress Brazil 2021. São Paulo. Anais…. São Paulo, 2021. https://iah2021brazil.org

FERNANDES, A.J.; MALDANER, C.H.; NEGRI, F.; ROULEAU, A.; WAHNFRIED, I.D. Aspects of a conceptual groundwater flow model of the Serra Geral basalt aquifer (Sao Paulo, Brazil) from physical and structural geology data. Hydrogeol J 24:1199–1212, 2016. https://doi.org/10.1007/s10040-016-1370-6

FIUME, B.; FERNANDES, A.J.; BARBOSA, M.B.; HIRATA, R.; BERTOLO, R.A. Integrated application of geophysical loggings and fracture survey on rock exposures for identifying transmissive fractures in crystalline aquifer: case study in the city of São Paulo. Brazilian Journal of Geology, 50, 2020. DOI: https://doi.org/10.1590/2317-4889202020190034

FRANK, H.T.; GOMES, M.E.B.; FORMOSO, M.L.L. Review of the areal extent and the volume of the Serra Geral Formation, Paraná Basin, South America. Pesquisas Geosci 36(1):49–57, 2009.

GARDIMAN JUNIOR, B.S.; MAGALHÃES, I.A.L.; FREITAS, C.A.A.; CECÍLIO, R.A. Análise de técnicas de interpolação para espacialização da precipitação pluvial na bacia do rio Itapemirim (ES). Revista do Setor de Ciências Agrárias e Ambientais 8(1):61-71, 2012.DOI:10.5777/ambiencia.2012.01.05

GOMES, M.G.; DE VARGAS, T.; BELLADONA, R.; DAL BOSCO, V.; DE ARAÚJO, B.; BORTOLIN, T.A. A vulnerabilidade natural de aquíferos fraturados: avaliando os modelos DRASTIC e GOD, originais e adaptados. Geociências, v. 40, n. 3, p. 735 - 749, 2021.

GUERRA, P.A.G. Geoestatística operacional. Departamento Nacional de Produção Mineral. 145p, 1988.

HALLAK, R. & PEREIRA FILHO, A.J. Metodologia para análise de desempenho de simulações de sistemas convectivos na região metropolitana de São Paulo com o modelo ARPS: sensibilidade a variações com os esquemas de advecção e assimilação de dados. Revista Brasileira de Meteorologia 26(4):591 – 608, 2011.

HERNANDEZ-STEFANONI, J.L. & PONCE-HERNANDEZ, R. Mapping the spatial variability of palnt diversity in a tropical forest: comparison of spatial interpolation methods. Environmental Monitoring and Assessment 117:307-334, 2006. DOI: 10.1007/s10661-006-0885-z.

HERNANDEZ, P.G.L.; ATHAYDE, G.B.; ATHAYDE, C.V.M.; LICHT, O.A.B. Effect of the interpolation of hydrogeological data in sedimentary aquifers: a case study in the state of Paraná. Águas Subterrâneas, v. 35, n. 1, p. 1-11, 2020.

IBGE – INSTITUTO BRASILEIRO DE GEOGRAFIA E ESTATÍSTICA. Project RADAMBRASIL: Folha SH.22 Porto Alegre and folhas SH.21 Uruguaiana and SI. 22 Lagoa Mirim: geologia, geomorfologia, pedologia, vegetação, uso potencial da terra. Rio de Janeiro – RJ, Vol. 33, 791 p, 1986.

JAKOB, A.A.E. & YOUNG, A.F. O uso do método de interpolação espacial das análises sociodemográficas. IN: XV ENCONTRO NACIONAL DE ESTUDOS POPULACIONAIS, Caxambu-MG: ABEP, p. 1-22, 2006.

KISAKA, M.O.; MUCHERU-MUNA, M.; NGETICH, F.K.; MUGWE, J.; MUGENDI, D.; MAIRURA, F.; SHISANYA, C.; MAKOKHA, G.L. Potential of deterministic and geostatistical rainfall interpolation under high rainfall variability and dry spells: case of Kenya's Central Highlands. Theor Appl Climatol 124:349-364, 2016. DOI: 10.1007/s00704-015-1413-2.

LANDIM, P.M.B. Introdução aos métodos de estimação espacial para confecção de mapas. DGA, IGCE, UNESP/Rio Claro, Lab. Geomatemática, Texto Didático 02, 20p, 2000. Available via DIALOG. http://www.sorocaba.unesp.br/Home/Graduacao/En genhariaAmbiental/robertowlourenco/dicas-surfer-01.pdf . Acessed June 2018.

LISBOA, N.A.; REMUS, M.V.D.; DANI, N.; CASTRO, J.W.; NETO, F.T. (Coordenadores). Estudo geológico e hidrogeológico para o aproveitamento de água do aquífero guarani no município de Caxias do Sul. Caxias do Sul: Relatório Final (Prefeitura Municipal de Caxias do Sul). 72p, 2003.

LIU, D.; WANG, Z.; ZHANG, B.; SONG, K.; LI, X.; LI, J. Spatial distribution of soil organic carbon and analysis of related factors in croplands of the black soil region, northeast China. Agriculture, Ecosystems & Environment 113:73-81, 2006. DOI: 10.1016/j.agee.2005.09.006.

MACHADO, J.L.F. & FREITAS, M.A. Projeto mapa hidrogeológico do Rio Grande do Sul: Relatório Final. Porto Alegre: CPRM, 2005.

MELFI, A.J.; PICCIRILLO, E.M.; NARDY, A.J.R. Geological and magmatic aspects of the Paraná Basin an introduction. In: PICCIRILLO, E.M. & MELFI, A.J. (Coordenadores.) The Mesozoic Flood Volcanism of the Paran_a Basin: Petrogenetic and Geophysical Aspects. IAG-USP, pp. 1-13, 1988.

MENDES, M.P. & RIBEIRO, L. Nitrate probability mapping in the northern aquifer alluvial system of the river Tagus (Portugal) using Disjunctive Kriging. Science of the Total Environment 408:1021–1034, 2010. DOI: 10.1016/j.scitotenv.2009.10.069.

MENG, Q.; LIU, Z.; BORDERS, B.E. Assessment of regression kriging for spatial interpolation-comparisons of seven GIS interpolation methods. Cartography and Geographic Information Science 40.1:p28+, 2013. DOI: http://dx.doi-org.ez45. periodicos.capes.gov.br/10.1080/15230406.2013.762138.

MORIASI, D.N.; ARNOLD, J.G.; VAN LIEW, M.W.; BINGNER, R.L.; HARMEL, R.D.; VEITH, T.L. Model evaluation guidelines for systematic quantification of accuracy in watershed simulations. Transactions of the ASABE 50(3): 885-900, 2007. DOI: http://citeseerx.ist.psu.edu/viewdoc/download?doi=10.1.1.532.2506&rep=rep1&type=pdf.

MUÑOZ-PARDO, J.F. & GARCIA, R. Estimation of the transmissivity of the Santiago aquifer, Chile, using different geostatistical methods. Groundwater Management: Quantity and Quality (Proceeding of the Benidorm Symposium). IAHS Publ. nº 188, 1989.

NOBRE, J.G.A.; TEIXEIRA, A.S.; SOUSA, V.F.; MOREIRA, L.C.J.; COSTA, C.A.; SIG como ferramenta de planejamento de uso de águas subterrâneas no município de Santa Rosa do Piauí-PI. In: XIV SIMPÓSIO BRASILEIRO DE SENSORIAMENTO REMOTO, 2009, Natal, Brasil. INPE, 4789-4795.

ÖZDAMAR, L.; DEMIRHAN, M.; ÖZPINAR, A. A comparison of spatial interpolation methods and a fuzzy areal evaluation scheme in environmental site characterization. Computers, Environment and Urban Systems 23:399-422, 1999.

PICADA, R.S. Ensaio sobre a tectônica do Escudo Sul-riograndense. In: CONGRESSO BRASILEIRO DE GEOLOGIA, 25. Anais. São Paulo. 1:167 – 191, 1971.

PIDWIRNY, M. Introduction to the Atmosphere. In: PIDWIRNY, M. Fundamentals of Physical Geography, 2nd Edition, 2006. http://www.physicalgeography.net/fundamentals/7d.html

PIELKE SR, R.A. Mesoscale Meteorological Modeling. 2nd edn. International Geophysics Series. EUA, Academic Press, v. 78. 676p, 2002.

RAZACK, M. & LASM, T. Geostatistical estimation of the transmissivity in a highly fractured metamorphic and crystalline aquifer (Man-Danane Region, Western Ivory Coast). Journal of Hydrology 325:164-178, 2005. DOI: 10.1016/j.jhydrol.2005.10.014

REGINATO, P.A.R. Integração de Dados para Prospecção de Aquíferos Fraturados em Trecho da Bacia Hidrográfica Taquari - Antas (RS). Doctoral thesis. Postgraduate Program in Mining, Metallurgical and Materials Engineering – PPGEM. Engineering Institute. Federal University of Rio Grande do Sul, 254 p, 2003.

REGINATO, P.A.R. & STRIEDER, J.A. Integration of geologic data in the prospection of fractured aquifer at the Serra Geral Formation. Águas Subterrâneas 20:1–14, 2006.

ROISENBERG, A. & VIERO, A.P.O. Vulcanismo Mesozóico da Bacia do Paraná no Rio Grande do Sul. In: HOLZ, M. & DE ROS, F. (Coordenadores) Geologia do Rio Grande do Sul. CIGO/UFRGS, Porto Alegre, Brazil, pp 355–374, 2000.

ROSSATO, M.S. Os climas do Rio Grande do Sul: variabilidade, tendências e tipologia. Doctoral thesis - Postgraduate Program in Geography, Institute of Geosciences, Federal University of Rio Grande do Sul, 240 p, 2011.

SAJID, A.H.; RUDRA, R.P.; PARKIN, G. Systematic evaluation of kriging and inverse distance weighting methods for spatial analysis of soil bulk density. Canadian Biosystems Engineering 55, 2013. DOI: http://dx.doi.org/10.7451/CBE.2013.55.1.1

SARAIVA, G.S.; BONOMO, R.; SOUZA, J.M. Avaliação de interpoladores geoestatísticos e determinísticos da evapotranspiração de referência diária para o estado do Espírito Santo. Revista Agroambiente On-line 11(1):21-30, 2017. DOI: 10.18227/1982-8470ragro.v11i1. 3647.

SILVA, J.L.S.; FILHO, L.L.V.D.; LORENSI, R.P.; CRUZ, J.C.; ELTZ, F.L.F. Vulnerability of the Serra Geral aquifer to contamination in the city of Erechin. Revista Ciência e Natura 35(1): 010-023, 2013. DOI: http://dx.doi.org/10.5902/2179-460X07.

SYED, A.R. A review of cross validation and adaptive model selection. Master of Science in the College of Arts and Sciences Georgia State University. Department of mathematics and statistics. Georgia State University, 26 p, 2011.

TADIĆ, J.M.; ILIĆ, V.; BIRAUD, S. Examination of geostatistical and machine-learning techniques as interpolators in aniso-tropic atmospheric environments. Atmospheric Environment 111:28-38, 2015. DOI: http://dx.doi.org/10.1016/j.atmosenv.2015. 03.063

VARGAS, T.; ADAMI, M.V.D.; AVER, E.A.S.; BELLADONA, R.; ZAGO, M.A.; FRIZZO, E.E. Monitoramento hidroquímico dos córregos afluentes da represa Faxinal, Caxias do Sul – RS. In: XX SIMPÓSIO BRASILEIRO DE RECURSOS HÍDRICOS, 2013, Bento Gonçalves – RS. Available via DIALOG. https://www.

abrh.org.br/SGCv3/index.php?BUSCA=ARTIGOS&iPUB=3 &Q=Monitoramento%20hidroqu%C3%ADmico%20dos%20c %C3%B3rregos%20afluentes%20. Acessed August 2014.

VARGAS, T.; GOMES, M.G.; BELLADONA, R.; ADAMI, M.V.D. Aplicação do Interpolador IDW para Elaboração de Mapas Hidrogeológicos Paramétricos na Região da Serra Gaúcha. Scientia Cum Industria, 6(3)38 – 43, 2018. DOI: http://dx.doi.org/10.18226/23185279.v6iss3p38

YAMAMOTO, J.K. & LANDIM, P.M.B. Geoestatística: conceitos e aplicações. Ed. Oficina de Textos. São Paulo, 2013.

YAO, L.; HUO, Z.; FENG, S.; MAO, X.; KANG, S.; CHEN, J.; XU, J.; STEENHUIS, T.S. Evaluation of spatial interpolation methods for groundwater level in an arid inland oasis, northwest China. Environ Earth Sci 71:1911-1924, 2014. DOI: 10.1007/s12665-013-2595-5.

WILLMOT, C.J. Some Comments on the Evaluation of Model Performance. Bulletin of the American Meteorological Society 63:1309-1313, 1982.